HIGH SPEED FLOW SIMULATIONS USING UNSTRUCTURED ADAPTIVE GRIDS

Heidi Korzenowski
UNIVAP – Universidade do Vale do Paraíba, Instituto de Pesquisa e Desenvolvimento, 12244-000, São José dos Campos, SP, Brasil. E-mail: heidi@univap.br

Abstract

A high-resolution flux-vector splitting scheme is used to obtain the solution over a blunt hypersonic body. The numerical simulations are concerned with the implementation of unstructured grid, mesh refinement techniques for two-dimensional inviscid fluid flow. The governing equations are discretized in a cell centered, finite volume procedure. Spatial discretization considered a second-order flux-vector splitting scheme. A MUSCL extrapolation of primitive variables is used in order to determine left and right states at the interfaces. An adaptive mesh refinement procedure, based on a sensor of flow property gradients, is performed to obtain a better resolution of strong discontinuities. Results for different freestream Mach number are obtained in order to determine by analysis the constitution of some phenomena presented in such high-speed flow.

Key words: adaptive mesh, unstructured grid, finite volume method

1. INTRODUCTION

The development of efficient numerical solvers is very important owing to the difficulties and high costs associated with the experimental work at high speed flows. The hypersonic fluid flow simulation over a blunt-nosed body is characterized by a strong detached shock ahead the body. This phenomenon is particularly interesting because the curved bow shock is a normal shock wave in the nose region, and away from this one has all possible oblique shock solutions for a given freestream Mach number. A good capture of fluid flow features is obtained by use of an appropriate refined mesh and an efficient fluid solver. The introduction of mesh adaptivity reduces the number of grid elements because the regions that need to be refined are small compared with the size of the complete computational domain. Therefore, one can reduce storage and CPU requirements by the use of adaptive refinement, when compared with a fixed fine mesh, which would yield the same resolution of the relevant flow features. Some strategies to determine the mesh refinement have been derived (Sonar, 1995; Marcum, 1995). In this work, a numerical sensor based on gradients of flow properties determines the regions that need to be refined.

A finite volume formulation of compressible Euler equations in conservative form has been considered. A high-resolution scheme is employed in order to obtain a good spatially resolution of the flow features. Many numerical upwind methods have been derived (van Leer, 1982; Osher, 1985). In this work the simulations are performed by using an $AUSM^+$ scheme (Liou, 1994). Liou states that this scheme achieve high accuracy over a wide range of problems described by Euler and Navier-Stokes equations.

The second-order AUSM$^+$ scheme is implemented in an unstructured grid context (Azevedo and Korzenowski, 1998). In this approach, the convective operator can be expressed as a sum of the convective and pressure terms. This scheme considers a MUSCL approach (Hirsh, 1990), that is, the interface fluxes are formed using left and right states at the interface, which are linearly reconstructed by primitive variable extrapolation on each side of the interface. The Euler equations are discretized in a cell centered based finite volume procedure on triangular meshes. Time march uses an explicit, 2nd-order accurate, five-stage Runge-Kutta time stepping scheme (Mavriplis, 1988).

The hypersonic flow simulations are performed over a blunt-nosed body. The freestream Mach number were varied from M_∞=10 until M_∞=20. The fluid was treated as a perfect gas, and no chemistry was taken into account. The shock detachment distance obtained by numerical solutions was compared with the shock detachment distance estimated by Byllig's correlation (Billig, 1967). Results indicate that the scheme could adequately capture the flowfield features.

2. THEORETICAL FORMULATION

The 2-D time-dependent Euler equations, in conservative form, can be written as

$$\frac{\partial}{\partial t}\int_V Q\,dV + \int_S (E dy - F dx) = 0\,, \tag{1}$$

where V represents the area of the control volume and S is its boundary. Expressions for the vector of conserved quantities, Q, and the convective flux vectors, E and F, are found in Azevedo and Korzenowski (1998).

If the equations are discretized using a cell centered based finite volume procedure, the discrete vector of conserved variables, Q_i, is defined as an average over the i-th control volume. In this context, the flow variables can be assumed as attributed to the centroid of each cell. The Equation (1) can then be rewritten for the i-th volume as

$$\frac{\partial}{\partial t}(V_i Q_i) + \int_S (E dy - F dx) = 0\,. \tag{2}$$

3. SPATIAL DISCRETIZATION ALGORITHM

The spatial discretization is concerned with finding a discrete approximation to the surface integral in Equation (2). This approximation is essentially the convective operator, $C(Q_i)$.

The numerical fluxes E and F can be expressed as the sum of the numerical convective flux and the numerical pressure flux at each cell interface (Liou, 1996). Therefore, the numerical convective flux is defined in terms of Mach number, speed of sound and the quantity Φ, defined as $\Phi = (\rho, \rho u, \rho v, \rho H)^T$. For the AUSM$^+$ formulation, the Mach number and the pressure are splitting accordingly some properties, as described in Liou (1996).

The second-order method uses a MUSCL approach for the extrapolation of primitive variables. By this approach, left and right states at a given interface are linearly reconstructed

by primitive variable extrapolation on each side of the interface, together with some appropriate limiting process in order to avoid the generation of new extreme. In order to reconstruct interface properties, the unstructured grid case considers a local one-dimensional stencil normal to the edge considered.

The Liou scheme implemented in this work considers that the convective operator can be expressed as a sum of the convective and pressure terms, given by the expression.

$$C(Q_i) = (F_{ik}^{(c)} + P_{ik})\ell_{ik}\,, \tag{5}$$

where ℓ_{ik} represents the length of the ik edge. Expressions of the terms $F_{ik}^{(c)}$ and P_{ik}, as well as details of the formulations can be found in Azevedo and Korzenowski (1998).

4. BOUNDARY CONDITIONS

The implementations of the boundary conditions were performed by using ghost cells. Three types of boundary conditions were considered in the simulations over a hypersonic body. They are entrance, wall and exit boundary conditions.

At the wall boundary, the flow must be tangent to the wall in the inviscid case. This is done by imposing that the velocity component normal to the wall in the ghost volume has the same magnitude and opposite sign of the normal velocity component in its adjacent interior volume, whereas the ghost volume velocity component tangent to the wall is exactly equal to its internal cell. Besides, a zero normal pressure gradient and a zero normal temperature gradient at the wall is assuming.

For supersonic/hypersonic flow, all quantities at the entrance must be given. In the present work, all flow properties are dimensionless. At the supersonic exit, all boundary quantities are obtained by extrapolation of interior information.

5. GRID GENERATION AND ADAPTATION

The grid generation process is based on Pirzadeh (1993). In this approach a grid is generated by forming cells starting from the domain boundaries and marching toward the interior of the computational domain. The local grid characteristics, such as grid point distribution, are controlled by information stored at the nodes of a secondary coarse mesh referred as the background grid. The background grid consists of a structured grid that that encloses the entire domain without the requirement of conforming to the configuration. Its function is to guide a marching front for insertion of new points at proper locations. As the front advances into the field, the grid parameters defining the position of a new point are interpolated from the values stored at the nodes of the background grid cell that encloses the point.

The adaptive mesh refinement implemented in this work uses a sensor based on gradients of flow properties, which identify the regions that require grid refinement. The process consists of two steps. The first one is to compute the flow on an existing coarse mesh. With this preliminary solution, one can calculate the sensor for all triangles. All marked triangles are refined. A new finer mesh is then constructed by enrichment of the original grid.

The mesh enrichment procedure introduces an additional node for each side of the triangle marked by refinement. Then, the code has to search all triangles to identify cells that have two or three divided sides. Each of these cells is subdivided into four new triangles. This subdivision may eventually mark new faces. Therefore, this process has to be performed until

there are no triangles with more than one marked face. In order to avoid hanging nodes, the triangles that have one marked face should be divided by halving.

The second step of the refinement process consists of identifying all triangles which were refined by halving. This information is stored for the next refinement step because, if there is again an attempt to subdivide these triangles by halving, this is not allowed. Therefore, if the next refinement step tries to divide by halving a triangle which was obtained by a previous division by halving, the logic in the code forces the original triangle to be divided into four new triangles before the refinement procedure is allowed to continue. When the mesh enrichment procedure has been completed, the new control volumes receive the property values of their "father" triangle and the flow solver is re-started.

6. RESULTS AND DISCUSSION

A blunt-nosed body was used to obtain the hypersonic fluid flow simulations. Although simulations were performed for M_∞=10 to M_∞=20, only results for M_∞=20 were presented. The adaptive mesh adopted in the present simulations was obtained with one pass of refinement. This refined level was performed when the L_2 norm of the change in density variable drops over two order of magnitude. Typically, around 2000 iterations are required to satisfy this convergence criterion. The sensor was based on all primitive variable gradients.

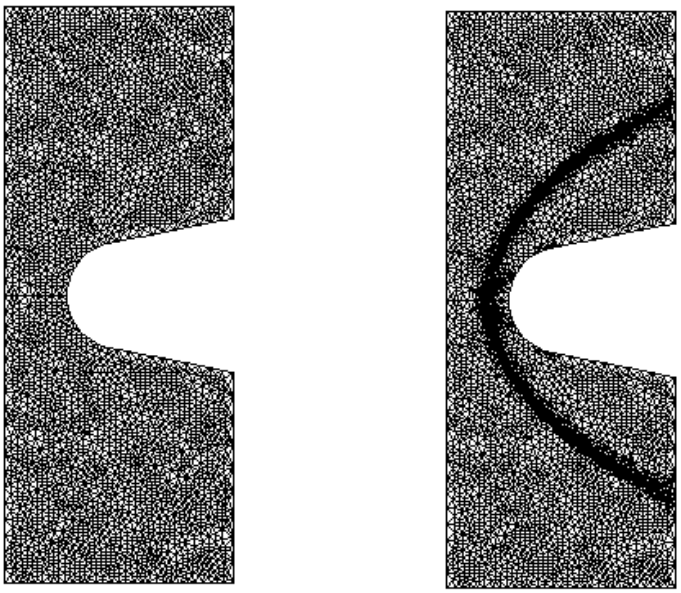

Figure 1. Initial and adaptive unstructured meshes used on simulations at M_∞=20.

Meshes with more than one adaptive refinement pass were generated, but the adoption of more refined grids resulted in a bad convergence behavior. No freezing of limiters was used here. The initial mesh has 6072 nodes and 11780 volumes, while the adaptive mesh is composed of 7124 nodes and 12968 volumes. The initial and final meshes are shown in Figure 1.

The Mach number contours obtained with the second-order Liou scheme are presented in Figure 2. The contours indicate that the flow features are well captured by this solution, the bow shock and the flow expansion over the body are well represented. One can see that at the nose of the body the shock is normal, and away from this the shock wave gradually becomes curved and weaker. The hypersonic flow ahead the shock becomes subsonic behind this one,

that is, there is a strong compression of the flow in this region. Slightly above the nose region, the shock is oblique and pertains to the strong shock-wave solution. As we move further along the shock, the wave angle becomes more oblique, and the flow deflection decreases until reach the maximum deflection angle. From the nose region until this point the flow is subsonic. Above this one, all points on the shock correspond to the weak shock solution. This region is characterized by supersonic flow.

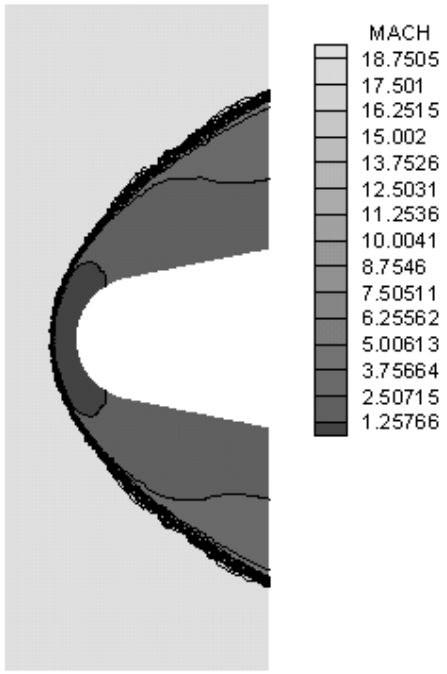

Figure 2. Mach contours obtained with the Liou scheme at M_∞=20.

The streamline that passes through this normal portion of the shock impinges on the nose of the body and controls the values of stagnation pressure and temperature at the nose. The pressure and the density contours are plotted in Figure 3.

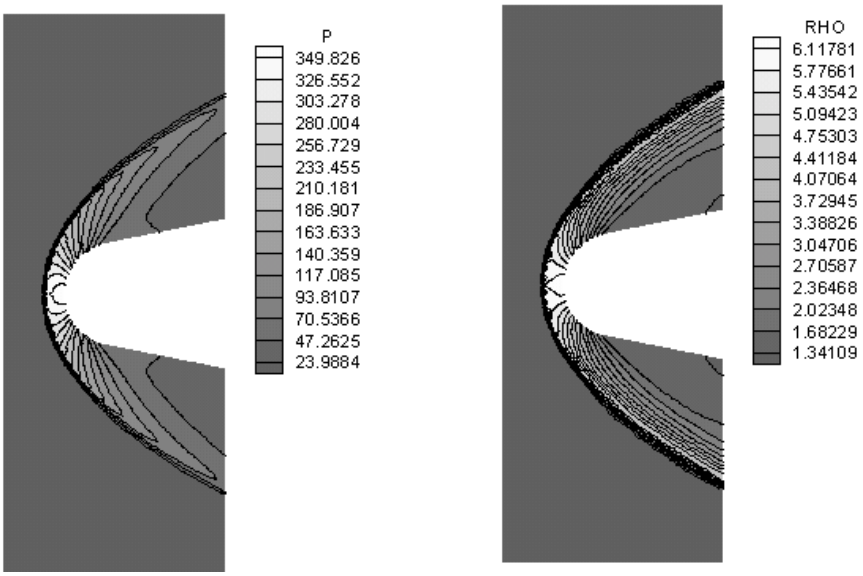

Figure 3. Pressure and density contours obtained with the Liou's scheme at M_∞=20.

The contours indicate that the flow features are well captured by the Liou's AUSM$^+$ scheme can be observed in Figure 3. The oscillations presented in the strong shock ahead the body, observed in Mach and density contours, can be improvement by use of a more refined mesh. However, one has some difficulties to obtain convergence to machine zero with refined meshes, as one still explains.

The pressure and density downstream of the wave, obtained by use of the basic normal shock equations, are $p_2 = 33322$ and $\rho_2 = 5{,}926$, respectively. The properties obtained by the numerical simulations are $p_2 = 34982$ and $\rho_2 = 6{,}11$. One can observe a minimal error between the analytical and numerical results, indicating that the scheme was adequate to assess the properties of the flow.

The shock detachment distance obtained by numerical solutions is 0,12m, and the shock detachment distance estimated by Byllig's correlation gives 0,05m. Figure 4 shows the Mach number contours along the centerline and the shock location given by the correlation. One can see the difference between these two approaches.

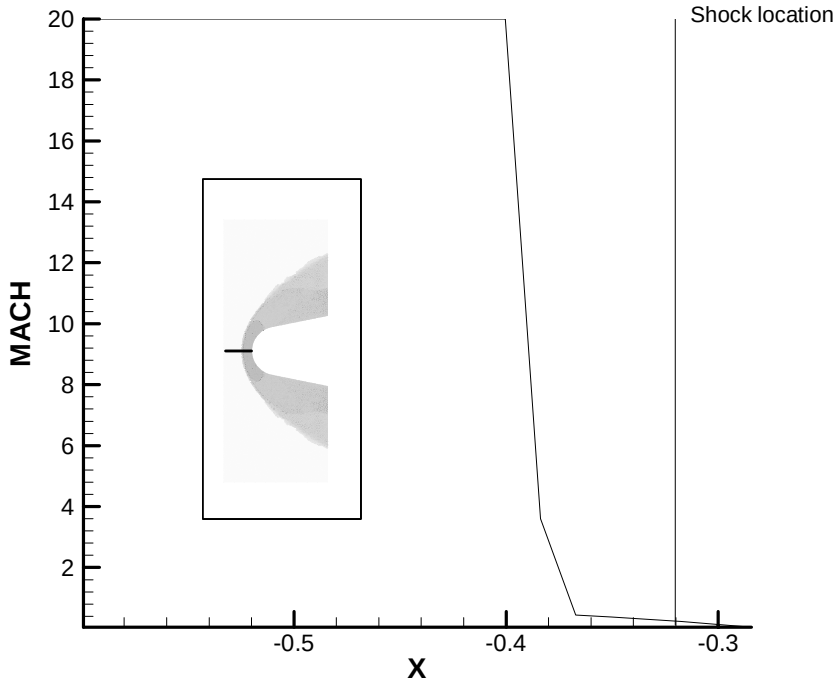

Figure 4. Computed Mach number on centerline surface.

Although the numerical shock location does not agree with the correlation, this result makes some sense, because the simulations were performed considering that the fluid is a perfect gas. If real gas effects are incorporated into computational solver, the shock location will place nearer to the body. Results for reactive flow simulations can be found in Drikakis and Tsangaris (1993).

7. CONCLUDING REMARKS

The present work performed hypersonic flow simulations over a blunt body. The governing equations are discretized in an unstructured triangular mesh by a cell centered finite volume algorithm. The spatial discretization considers an $AUSM^+$ flux-vector splitting scheme. A MUSCL reconstruction of primitive variables was used in order to obtain left and right states at interfaces. The equations are advanced in time by an explicit, 5-stage, 2^{nd}-order accurate, Runge-Kutta time stepping procedure.

An inviscid formulation was used and the fluid was treated as a perfect gas. The solver has been coupled with a mesh adaption algorithm. The adaptive refinement procedure uses a sensor based on gradients of flow properties. The mesh generation introduces new points automatically into computational domain by advancing front generation.

Results obtained with one pass of adaptive refinement are presented. Although the simulations could capture all flow features with good accuracy, more refined mesh are employed.

7.1 Acknowledgments

The author would like to acknowledge the support received from FAPESP through a Research Grant No. 98/09812-6.

8. REFERENCES

- Azevedo, J.L.F., Korzenowski, H., 1998, "Comparison of Unstructured Grid Finite Volume Methods for Cold Gas Hypersonic Flow Simulations", AIAA Paper 98-2629, pp. 447-463.
- Billig, F.S., 1967, "Shock-Wave around Spherical- and Cylindrical-Nosed Bodies", Journal of Spacecraft, Vol. 4, No.6, pp. 822-823.
- Drikakis, D., Tsangaris, S., 1993, "On The Accuracy and Efficiency of CFD Methods in Real Gas Hypersonics", International Journal for Numerical Methods in Fluids, Vol. 16, pp. 759-775.
- Hirsh, C., 1990, *Numerical Computation of Internal and External Flows. Vol. 2: Computational Methods for Inviscid and Viscous Flows*, Wiley, New York.
- Liou, M.-S., 1994, "A Continuing Search for a Near-Perfect Numerical Flux Scheme. Part I: AUSM", NASA TM-106524, NASA Lewis Research Center, Cleveland, OH.
- Liou, M.-S., 1996, "A Sequel to AUSM: AUSM", Journal of Computational Physics, Vol. 129, pp. 364-382.
- Marcum, D.L., 1995, "Adaptive Unstructured Grid Generation for Viscous flow Applications", AIAA Journal, Vol. 34, No. 11, pp. 2440-2443.
- Mavriplis, D.J., 1988, "Multigrid solution of the two-dimensional Euler equations on Unstructured Triangular Meshes, AIAA Journal, Vol. 26, No. 7, pp. 824-831.
- Osher, S., "Convergence of Generalized MUSCL Schemes", SIAM Journal Numerical Analysis", Vol. 22, No. 5.
- Pirzadeh, S., "Structured Background Grids for Generation of Unstructured Grids by Advancing-Front Method", AIAA Journal, Vol. 31, No. 2, pp. 257-265.
- Sonar, T., 1992, "Dem Fehler auf der Spur", DLR-Nachrichten, Heft 78, pp. 7-14.
- van Leer, B., 1995, "Flux-Vector Splitting for the Euler Equations", Proceedings of the 8^{th} International Conference on Numerical Methods in Fluid Dynamics, E. Krause, editor, Lecture Notes in Physics, Vol. 170, pp. 507-512.